PCCP

Cite this: *Phys. Chem. Chem. Phys.*, 2012, **14**, 11994–11998

www.rsc.org/pccp

PAPER

Manipulation of molecular rotational dynamics with multiple laser pulses

Shian Zhang,* Chenhui Lu, Tianqing Jia and Zhenrong Sun

Received 4th December 2011, Accepted 19th June 2012
DOI: 10.1039/c2cp23850k

In this paper, a theoretical model is proposed to investigate the molecular rotational state populations pumped by multiple laser pulses through an impulsive Raman process based on second-order perturbation theory and an analytical solution for the dependence of the rotational state populations on the time delays and the relative amplitudes of the multiple laser pulses has been achieved. The results indicate that the molecular rotational state populations can be controlled by precisely manipulating the time delays and the relative amplitudes, which can be significantly enhanced or completely suppressed, and so the molecular rotational wave packet and field-free molecular alignment can be efficiently manipulated.

Introduction

When a laser pulse is applied to a molecule, a rotational wave packet in the molecular vibronic ground state can be created. The production of the rotational wave packet induced by the laser field will lead to molecular alignment along the laser polarization direction.[1–4] The laser-induced molecular alignment can be obtained in both adiabatic and non-adiabatic regimes.[2] In an adiabatic process, the molecular alignment occurs under the laser field and will vanish when the laser pulse is off. In a non-adiabatic process, the molecular alignment is maximally obtained after the laser pulse and periodically reconstructed at the full of the molecular rational period and so it results in field-free molecular alignment. Recently, field-free molecular alignment has attracted considerable attention for its applications in molecular frame photoelectron angular distribution,[5,6] high-order harmonic generation,[7,8] molecular orbital imaging[9] and intense laser pulse propagation.[10–12] The dynamics of field-free molecular alignment can be controlled by applying two or multiple time-delayed laser pulses,[13–21] which can be significantly enhanced or completely suppressed by precisely manipulating their intensity ratios and time delays.

The molecular rotational wave packet is built by populating the rotational states through an impulsive Raman process and therefore the rotational state populations can directly reflect the amplitude of the rotational wave packet. If the rotational state populations can be manipulated by the laser field, the rotational wave packet can be controlled and therefore results in field-free molecular alignment. In this paper, based on second-order perturbation theory, we theoretically investigate the molecular rotational state populations pumped by multiple laser pulses through an impulsive Raman process and an analytical solution for the dependence of the rotational state populations on the time delays and relative amplitudes of the multiple laser pulses has been achieved. With three laser pulses as an example, we show that the molecular rotational state populations can be significantly enhanced or completely suppressed by precisely manipulating their time delays and relative amplitudes and so the rotational wave packet and field-free molecular alignment can be coherently controlled.

We consider multiple time-delayed laser pulses with the same linear polarization direction, given by

$$E(t) = E_1(t_1) + E_2(t_2) + E_3(t_3) + \cdots + E_i(t_i), \qquad (1)$$

where $E_i(t_i) = A_i\exp(-2\ln 2t_i^2/\tau^2)\cos(\omega t_i)$ and $t_i = t_1 - \sum_{j=2}^{i} T_{\mathrm{d}j}$, $T_{\mathrm{d}j}$ is the time delay between the j and $(j-1)$ laser pulses, A_i is the field amplitude, τ is the pulse duration and ω is the laser central frequency. As shown in Fig. 1, when a molecule is exposed to the laser field $E(t)$, the transition from the rotational states $|J\rangle$ to $|J+2\rangle$ is coupled through an impulsive Raman process. Based on second-order perturbation theory, the Raman transition probability can be approximated as[22,23]

$$\mathrm{P}_{J-J+2} \propto \left|\int_{-\infty}^{+\infty} E(\omega)E^*(\omega-\omega_J)\mathrm{d}\omega\right|^2, \qquad (2)$$

where $E(\omega)$ is the Fourier transform of $E(t)$, ω_J is the angular Raman frequency with $\omega_J = 2\pi(E_{J+2} - E_J)/\mathrm{h} = 2\pi\mathrm{cB}(4J+6) = (4J+6)\pi/T_{\mathrm{rot}}$, h is the Planck constant, c is the speed of the light, E_J is the energy of the J rotational state with $E_J = \mathrm{hcB}J(J+1)$, B is the molecular rotational constant, J is the rotational quantum number and T_{rot} is the molecular rotational period with $T_{\mathrm{rot}} = 1/(2\mathrm{Bc})$. It is noted that the high-frequency terms in eqn (2) are integrated to be zero when the laser frequency ω is much greater than the Raman frequency ω_J (*i.e.*, $\omega \gg \omega_J$) and

---

State Key Laboratory of Precision Spectroscopy, Department of Physics, East China Normal University, Shanghai 200062, People's Republic of China. E-mail: sazhang@phy.ecnu.edu.cn, zrsun@phy.ecnu.edu.cn

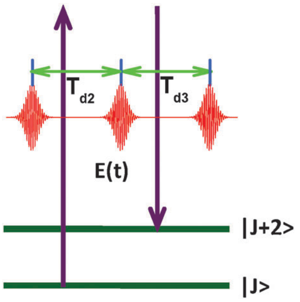

Fig. 1 A schematic diagram of the impulsive Raman transition from the rotational states $|J\rangle$ to $|J+2\rangle$, induced by the three time-delayed laser pulses.

thus the Raman transition probability P_{J-J+2} can be further simplified as

$$P_{J-J+2} \propto \left[1+\sum_i \gamma_i^2 \cos\left(\omega_J \sum_{j=2}^{i} T_{\mathrm{d}j}\right)\right]^2 + \left[\sum_i \gamma_i^2 \sin\left(\omega_J \sum_{j=2}^{i} T_{\mathrm{d}j}\right)\right]^2, \qquad (3)$$

where γ_i^2 is the relative amplitude with $\gamma_i^2 = (A_i/A_1)^2$. When the molecular ensemble in the thermal equilibrium is considered, the Raman transition probability P_{J-J+2} should be averaged over the Boltzmann distribution of the initial rotational states J, and so the total Raman transition probability P can be written as

$$P \propto \sum_J W_J^2 \left\{\left[1+\sum_{\mathrm{i}} \gamma_i^2 \cos\left(\omega_J \sum_{j=2}^{i} T_{\mathrm{d}j}\right)\right]^2 + \left[\sum_i \gamma_i^2 \sin\left(\omega_J \sum_{j=2}^{i} T_{\mathrm{d}j}\right)\right]^2\right\}, \qquad (4)$$

where W_J are the Boltzmann weight factors with $W_J = \exp[-\mathrm{B}J(J+1)/kT]/\mathrm{Q}$, Q is the rotational partition function, k is the Boltzmann constant and T is the molecular rotational temperature.

One can see from eqn (4) that the total Raman transition probability P depends on the time delays $T_{\mathrm{d}j}$ and the relative amplitudes γ_i^2 of the multiple laser pulses and therefore it can be controlled by precisely manipulating the time delays $T_{\mathrm{d}j}$ and the relative amplitudes γ_i^2. Here, we consider a simple and common case with three laser pulses and thus P can be controlled by varying the T_{d2} and T_{d3} time delays and the γ_2^2 and γ_3^2 relative amplitudes.

First, we studied the influence of the T_{d2} and T_{d3} time delays on the Raman transition probability P. To reduce the control parameters, we considered four special cases with the relative amplitudes $\gamma_2^2 = \gamma_3^2 = 1$, $1 + \gamma_2^2 = \gamma_3^2$, $1 + \gamma_3^2 = \gamma_2^2$ and $1 = \gamma_2^2 + \gamma_3^2$. That is to say, three laser pulses with the same intensities or one laser pulse that is equal to the sum of the other two laser pulses. Fig. 2 shows the contour plot of P, at the rotational temperature $T = 30$ K, as a function of the T_{d2} and T_{d3} time delays with the relative amplitudes $\gamma_2^2 = \gamma_3^2 = 1$ (a), $\gamma_2^2 = 0.5$ and $\gamma_3^2 = 1.5$ (b), $\gamma_2^2 = 1.5$ and $\gamma_3^2 = 0.5$ (c), and $\gamma_2^2 = \gamma_3^2 = 0.5$ (d). All data are normalized by P, induced by the first laser pulse, and hereafter the same method is used. As can be seen, P is strongly modulated by the T_{d2} and T_{d3} time delays. P is maximally enhanced at $T_{\mathrm{d2}} = T_{\mathrm{d3}} = T_{\mathrm{rot}}$ (labeled with circles), *i.e.*, the separation between two neighbouring laser pulses is the rotational period T_{rot}. P is completely suppressed at $T_{\mathrm{d2}} = T_{\mathrm{rot}}$ and $T_{\mathrm{d3}} = 0.5T_{\mathrm{rot}}$ for $\gamma_2^2 = 0.5$ and $\gamma_3^2 = 1.5$ (see Fig. 2(b)), $T_{\mathrm{d2}} = T_{\mathrm{d3}} = 0.5T_{\mathrm{rot}}$ for $\gamma_2^2 = 1.5$ and $\gamma_3^2 = 0.5$ (as shown in Fig. 2(c)) and $T_{\mathrm{d2}} = 0.5T_{\mathrm{rot}}$ and $T_{\mathrm{d3}} = T_{\mathrm{rot}}$ for $\gamma_2^2 = \gamma_3^2 = 0.5$ (as shown in Fig. 2(d), labeled with rectangles). Moreover, the manipulation of P can be obtained at any molecular rotational temperature (not shown here). These results indicate that three time-delayed laser pulses can provide an effective method to manipulate the molecular rotational state populations.

Next, we demonstrated the dependence of the Raman transition probability P on the relative amplitudes γ_2^2 and γ_3^2. Here, we only considered these representative time delays, labeled with circles and rectangles in Fig. 2. Fig. 3 shows the contour plot of P, at the rotational temperature $T = 30$ K, as a function of the relative amplitudes γ_2^2 and γ_3^2 with the $T_{\mathrm{d2}} = T_{\mathrm{d3}} = T_{\mathrm{rot}}$ (a), $T_{\mathrm{d2}} = T_{\mathrm{rot}}$ and $T_{\mathrm{d3}} = 0.5T_{\mathrm{rot}}$ (b), $T_{\mathrm{d2}} = T_{\mathrm{d3}} = 0.5T_{\mathrm{rot}}$ (c), and $T_{\mathrm{d2}} = 0.5T_{\mathrm{rot}}$ and $T_{\mathrm{d3}} = T_{\mathrm{rot}}$ (d) time delays. One can see that P can be enhanced but not suppressed at $T_{\mathrm{d2}} = T_{\mathrm{d3}} = T_{\mathrm{rot}}$ (as shown in Fig. 3(a)), while P can be enhanced or suppressed at $T_{\mathrm{d2}} = T_{\mathrm{rot}}$ and $T_{\mathrm{d3}} = 0.5T_{\mathrm{rot}}$ (as shown in Fig. 3(b)), $T_{\mathrm{d2}} = T_{\mathrm{d3}} = 0.5T_{\mathrm{rot}}$ (see Fig. 3(c)), and $T_{\mathrm{d2}} = 0.5T_{\mathrm{rot}}$ and $T_{\mathrm{d3}} = T_{\mathrm{rot}}$, (as shown in Fig. 3(d)). It can be found that P is completely suppressed when γ_2^2 and γ_3^2 satisfy the relation of $1 + \gamma_2^2 = \gamma_3^2$ or $1 + \gamma_3^2 = \gamma_2^2$ or $1 = \gamma_2^2 + \gamma_3^2$ (labeled with dashed lines), *i.e.*, one laser pulse is equal to the sum of the other two laser pulses. Consequently, we can conclude that P can be significantly enhanced or completely suppressed by precisely controlling the T_{d2} and T_{d3} time delays and the γ_2^2 and γ_3^2 relative amplitudes.

As mentioned previously, the rotational wave packet is generated in the initially populated rotational states through an impulsive Raman process. The rotational state populations (*i.e.*, P) can be manipulated by precisely controlling the T_{d2} and T_{d3} time delays and the γ_2^2 and γ_3^2 relative amplitudes of three laser pulses (as shown in Fig. 2 and 3) and so the rotational wave packet and therefore the field-free molecular alignment can be manipulated. To show the rotational wave packet or field-free molecular alignment can be manipulated by the three time-delayed laser pulses, we numerically solved the time-dependent Schrödinger equation based on a rigid-rotor model,[2]

$$i\hbar\frac{\partial|\Psi\rangle}{\partial t} = \left\{BJ(J+1) - \mu E(t)\cos\theta - \frac{1}{2}[(\alpha_\parallel - \alpha_\perp)\cos^2\theta + \alpha_\perp]E^2(t)\right\}|\Psi\rangle, \qquad (5)$$

where μ is the permanent dipole moment, θ is the angle between the molecular axis and the laser polarization and $\alpha_\parallel$ and $\alpha_\perp$ are the polarizability components parallel and perpendicular to the molecular axis, respectively. The molecular alignment degree or the rotational wave packet are characterized with the expectation value of $\cos^2\theta$ (*i.e.*, $\langle\cos^2\theta\rangle$) by considering the temperature-dependent Boltzmann distribution,

$$\langle\cos^2\theta\rangle = \sum_J W_J \sum_{M=-J}^{J} \langle\Psi_{JM}|\cos^2\theta|\Psi_{JM}\rangle. \qquad (6)$$

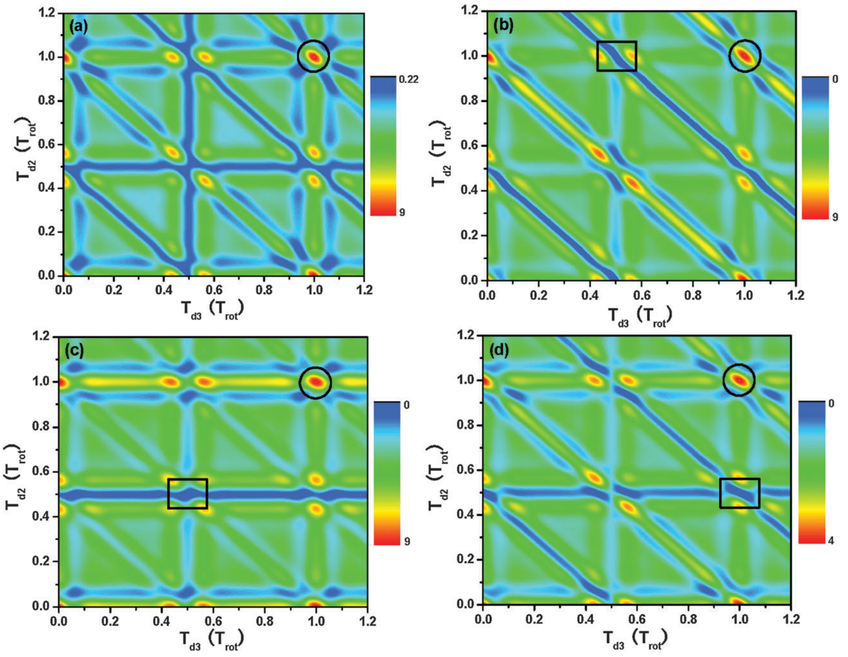

Fig. 2 A contour plot of the Raman transition probability P, at the rotational temperature T = 30 K, as a function of the T_{d2} and T_{d3} time delays with the relative amplitudes $\gamma_2^2 = \gamma_3^2 = 1$ (a), $\gamma_2^2 = 0.5$ and $\gamma_3^2 = 1.5$ (b), $\gamma_2^2 = 1.5$ and $\gamma_3^2 = 0.5$ (c), and $\gamma_2^2 = \gamma_3^2 = 0.5$ (d).

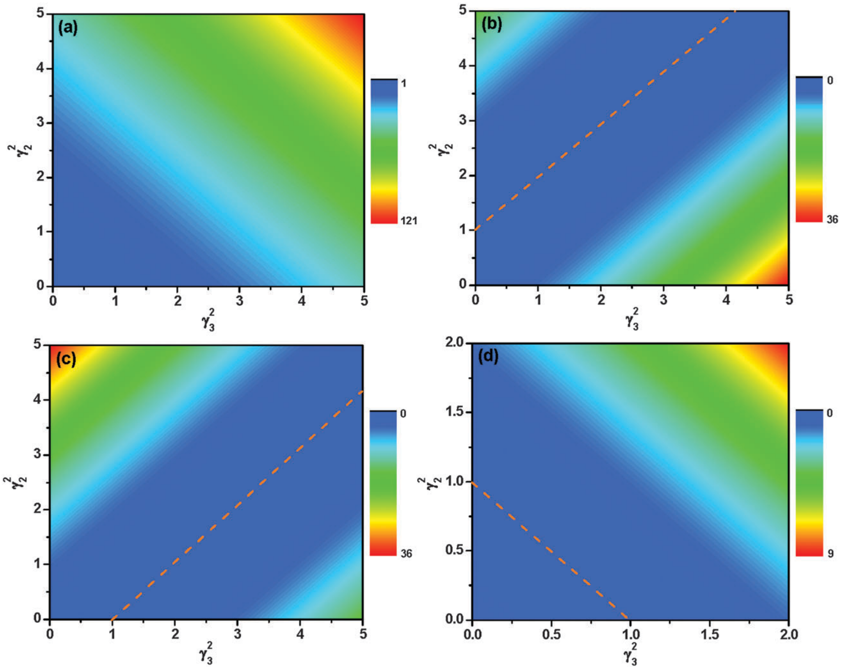

Fig. 3 A contour plot of the Raman transition probability P, at the rotational temperature T = 30 K, as a function of the γ_2^2 and γ_3^2 relative amplitudes with the time delays $T_{d2} = T_{d3} = T_{rot}$ (a), $T_{d2} = T_{rot}$ and $T_{d3} = 0.5T_{rot}$ (b), $T_{d2} = T_{d3} = 0.5T_{rot}$ (c), and $T_{d2} = 0.5T_{rot}$ and $T_{d3} = T_{rot}$ (d).

In our simulation, the time-dependent Schrödinger equation in eqn (5) is numerically calculated by a split operator method.[24] The CO molecule is used as an example and the molecular parameters are B = 1.93 cm^{-1}, μ = 0.112 D, $\alpha_{\parallel}$ = 2.294 Å^3 and $\alpha_{\perp}$ = 1.77 Å^3.[25–27] Here, the rotational period of the CO molecule can be calculated as $T_{rot} = 1/(2Bc)$ = 8.64 ps, its rotational temperature set to be 30 K and the central frequencies of all three laser pulses are 12 500 cm^{-1} with pulse durations of 200 fs.

Fig. 4 shows the time-dependent molecular alignment $\langle\cos^2\theta\rangle$ induced by the three laser pulses with time delays and relative amplitudes of $T_{d2} = T_{d3} = T_{rot}$ and $\gamma_2^2 = \gamma_3^2 = 1$ (a), $T_{d2} = T_{rot}$, $T_{d3} = 0.5T_{rot}$, $\gamma_2^2 = 0.5$ and $\gamma_3^2 = 1.5$ (b), $T_{d2} = T_{d3} = 0.5T_{rot}$, $\gamma_2^2 = 1.5$ and $\gamma_3^2 = 0.5$ (c), and $T_{d2} = 0.5T_{rot}$, $T_{d3} = T_{rot}$ and $\gamma_2^2 = \gamma_3^2 = 0.5$ (d). Here, the first laser pulse intensity is set to be 1 × 10^{13} W cm^{-2}. The three arrows are used to show three laser pulse positions and their length

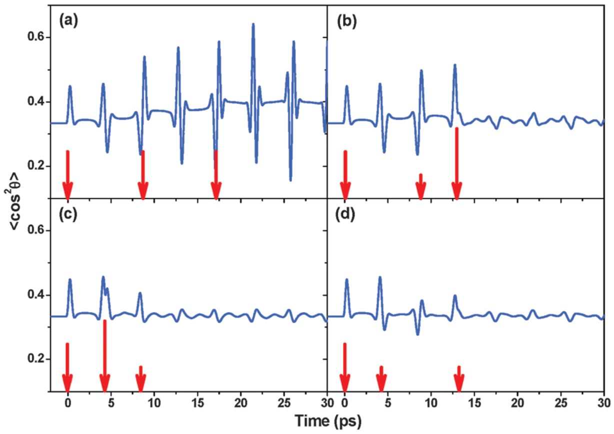

Fig. 4 The time-dependent molecular alignment $\langle\cos^2\theta\rangle$, at the rotational temperature T = 30 K, induced by three laser pulses with time delays and relative amplitudes of: $T_{d2} = T_{d3} = T_{rot}$ and $\gamma_2^2 = \gamma_3^2 = 1$ (a), $T_{d2} = T_{rot}$, $T_{d3} = 0.5T_{rot}$, $\gamma_2^2 = 0.5$ and $\gamma_3^2 = 1.5$ (b), $T_{d2} = T_{d3} = 0.5T_{rot}$, $\gamma_2^2 = 1.5$ and $\gamma_3^2 = 0.5$ (c) and $T_{d2} = 0.5T_{rot}$, $T_{d3} = T_{rot}$ and $\gamma_2^2 = \gamma_3^2 = 0.5$ (d). Here, the first laser intensity is set to be 1×10^{13} W cm^{-2}.

indicates their laser pulse intensities, respectively. One can see that $\langle\cos^2\theta\rangle$ is enhanced for $T_{d2} = T_{d3} = T_{rot}$ and $\gamma_2^2 = \gamma_3^2 = 1$ (as shown in Fig. 4(a)) and is almost completely suppressed for $T_{d2} = T_{rot}$, $T_{d3} = 0.5T_{rot}$, $\gamma_2^2 = 0.5$ and $\gamma_3^2 = 1.5$ (as shown in Fig. 4(b)), $T_{d2} = T_{d3} = 0.5T_{rot}$, $\gamma_2^2 = 1.5$ and $\gamma_3^2 = 0.5$ (as shown in Fig. 4(c)), and $T_{d2} = 0.5T_{rot}$, $T_{d3} = T_{rot}$ and $\gamma_2^2 = \gamma_3^2 = 0.5$ (as shown in Fig. 4(d)). Obviously, these observations are in good agreement with our previously mentioned predictions.

The Fourier transform of the molecular alignment signal can give the rotational state populations and therefore we can further observe the influence of the second and third laser pulses on the molecular rotational state populations induced by the first laser pulse. Fig. 5 shows the Fourier transform of the molecular alignment signal calculated in Fig. 4 (the solid lines), together with the difference from that induced only by the first laser pulse (the dashed lines). The positive value means that the second and third laser pulses can further enhance the rotational state populations and the negative value represents that the second and third laser pulses will suppress the rotational state populations. As can be seen, the rotational state populations are significantly enhanced when $T_{d2} = T_{d3} = T_{rot}$ and $\gamma_2^2 = \gamma_3^2 = 1$ (as shown in Fig. 5(a)) and are almost completely suppressed when $T_{d2} = T_{rot}$, $T_{d3} = 0.5T_{rot}$, $\gamma_2^2 = 0.5$ and $\gamma_3^2 = 1.5$ (as shown in Fig. 5(b)), $T_{d2} = T_{d3} = 0.5T_{rot}$, $\gamma_2^2 = 1.5$ and $\gamma_3^2 = 0.5$ (as shown in Fig. 5(c)) and $T_{d2} = 0.5T_{rot}$, $T_{d3} = T_{rot}$ and $\gamma_2^2 = \gamma_3^2 = 0.5$ (as shown in Fig. 5(d)). Therefore, these results are consistent with the previously mentioned calculations in Fig. 2 and 3.

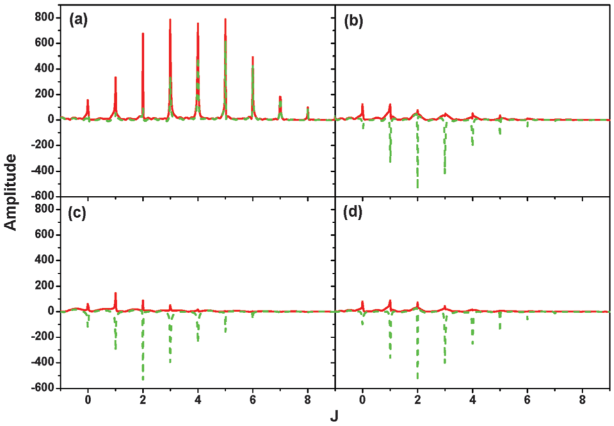

Fig. 5 The Fourier transform of the molecular alignment signal calculated in Fig. 4 (the solid lines), together with the difference to that induced only by the first laser pulse (the dashed lines).

Conclusions

In summary, we have presented a theoretical model to investigate the molecular rotational state population induced by multiple laser pulses through an impulsive Raman process, based on second-order perturbation theory, and an analytical solution for the dependence of the molecular rotational state populations on the time delays and the relative amplitudes of the multiple laser pulses is obtained. It shows that the molecular rotational state populations can be significantly enhanced or completely suppressed by precisely controlling the time delays and the relative amplitudes of the laser pulses and it can be further utilized to control the rotational wave packet and field-free molecular alignment.

Acknowledgements

This work was partly supported by the National Natural Science Fund (11004060 and 11027403) and the Shanghai Municipal Science and Technology Commission (10XD1401800, 09ZR1409300, 09JC1404700 and 10JC1404500).

References

1 H. Stapelfeldt and T. Seideman, *Rev. Mod. Phys.*, 2003, **75**, 543.
2 R. Torres, R. de. Nalda and J. P. Marangos, *Phys. Rev. A: At., Mol., Opt. Phys.*, 2005, **72**, 023420.
3 V. Loriot, P. Tzallas, E. P. Benis, E. Hertz, B. Lavorel, D. Charalambidis and O. Faucher, *J. Phys. B: At., Mol. Opt. Phys.*, 2007, **40**, 2503.
4 S. Guérin, A. Rouzée and E. Hertz, *Phys. Rev. A: At., Mol., Opt. Phys.*, 2008, **77**, 041404(R).
5 J. L. Hansen, L. Holmegaard, L. Kalhøj, S. L. Kragh, H. Stapelfeldt, F. Filsinger, G. Meijer, J. Küpper, D. Dimitrovski, M. Abu-samha, C. P. J. Martiny and L. B. Madsen, *Phys. Rev. A: At., Mol., Opt. Phys.*, 2011, **83**, 023406.
6 D. Dimitrovski, M. Abu-samha, L. B. Madsen, F. Filsinger, G. Meijer, J. Küpper, L. Holmegaard, L. Kalhøj, J. H. Nielsen and H. Stapelfeldt, *Phys. Rev. A: At., Mol., Opt. Phys.*, 2011, **83**, 023405.
7 C. Vozzi, F. Calegari, E. Benedetti, J.-P. Caumes, G. Sansone, S. Stagira, M. Nisoli, R. Torres, E. Heesel, N. Kajumba, J. P. Marangos, C. Altucci and R. Velotta, *Phys. Rev. Lett.*, 2005, **95**, 153902.
8 T. Kanai, S. Minemoto and H. Sakai, *Nature*, 2005, **435**, 470.
9 J. Itatani, J. Levesque, D. Zeidler, H. Niikura, H. Pépin, J. C. Kieffer, P. B. Corkum and D. M. Villeneuve, *Nature*, 2004, **432**, 867.
10 F. Calegari, C. Vozzi, S. Gasilov, E. Benedetti, G. Sansone, M. Nisoli, S. De Silvestri and S. Stagira, *Phys. Rev. Lett.*, 2008, **100**, 123006.
11 S. Varma, Y.-H. Chen and H. M. Milchberg, *Phys. Rev. Lett.*, 2008, **101**, 205001.
12 J. Wu, H. Cai, P. Lu, X. Bai, L. Ding and H. Zeng, *Appl. Phys. Lett.*, 2009, **95**, 221502.

13 K. F. Lee, I. V. Litvinyuk, P. W. Dooley, M. Spanner, D. M. Villeneuve and P. B. Corkum, *J. Phys. B: At., Mol. Opt. Phys.*, 2004, **37**, L43.

14 K. F. Lee, E. A. Shapiro, D. M. Villeneuve and P. B. Corkum, *Phys. Rev. A: At., Mol., Opt. Phys.*, 2006, **73**, 033403.

15 N. Xu, C. Wu, J. Huang, Z. Wu, Q. Liang, H. Yang and Q. Gong, *Opt. Express*, 2006, **14**, 4992.

16 Y. Gao, C. Wu, N. Xu, G. Zeng, H. Jiang, H. Yang and Q. Gong, *Phys. Rev. A: At., Mol., Opt. Phys.*, 2008, **77**, 043404.

17 C. Z. Bisgaard, M. D. Poulsen, E. Péronne, S. S. Viftrup and H. Stapelfeldt, *Phys. Rev. Lett.*, 2004, **92**, 173004.

18 C. Z. Bisgaard, S. S. Viftrup and H. Stapelfeldt, *Phys. Rev. A: At., Mol., Opt. Phys.*, 2006, **73**, 053410.

19 Y. Li, P. Liu, S. Zhao, Z. Zeng, R. Li and Z. Xu, *Chem. Phys. Lett.*, 2009, **475**, 183.

20 M. Leibscher, I. Sh. Averbukh and H. Rabitz, *Phys. Rev. Lett.*, 2003, **90**, 213001.

21 M. Leibscher, I. Sh. Averbukh and H. Rabitz, *Phys. Rev. A: At., Mol., Opt. Phys.*, 2004, **69**, 013402.

22 D. Meshulach and Y. Silberberg, *Phys. Rev. A: At., Mol., Opt. Phys.*, 1999, **60**, 1287.

23 M. Renard, E. Hertz, B. Lavorel and O. Faucher, *Phys. Rev. A: At., Mol., Opt. Phys.*, 2004, **69**, 043401.

24 J. Wu and H. Zeng, *Phys. Rev. A: At., Mol., Opt. Phys.*, 2010, **81**, 053401.

25 A. D. Bandrauk and H. Shen, *J. Chem. Phys.*, 1993, **99**, 1185.

26 K. A. Peterson and T. H. Dunning Jr., *J. Mol. Struct. (Theochem)*, 1997, **400**, 93.

27 M. Pecul, *Chem. Phys. Lett.*, 2005, **404**, 217.